

## **Investigation of the maximum Young's modulus of thyroid nodules using two-dimensional shear wave elastography in thyroid nodules.**

**Jing Hang<sup>1</sup>, Hai-yan Xue<sup>1</sup>, Hong-yan Deng<sup>1</sup>, Xin-hua Ye<sup>1</sup>, Cui-ying Li<sup>1</sup>, Wen-ting Ma<sup>1</sup>, Fan Li<sup>2</sup>, Lian-fang Du<sup>2\*</sup>**

<sup>1</sup>Department of Ultrasound, the First Affiliated Hospital with Nanjing Medical University, Nanjing, PR China

<sup>2</sup>Department of Ultrasound, Shanghai General Hospital of Nanjing Medical University, Shanghai, PR China

### **Abstract**

**Objective:** To investigate the maximum Young's modulus (SWE-max) of thyroid nodules using two-dimensional Shear Wave Elastography (2D-SWE) in thyroid nodules. Young's modulus is a measure of the stiffness of a solid material. It defines the relationship between stress (force per unit area) and strain (proportional deformation) in a material.

**Materials and method:** A total of 244 patients with 289 nodules scheduled for thyroid operation or fine-needle aspiration were recruited in our study. 2D-SWE examinations were performed after the grey-scale ultrasound to get the maximum Young's modulus of thyroid nodules, which were then correlated with pathology results. Then we investigate the distribution of the SWE-max by using logarithmic normal distribution. Finally we presented the association in differentiation the quality of thyroid nodules with the nodule's SWE-max.

**Result:** The mean age was  $45.58 \pm 12.15$  years old. Of all these 244 patients, 18 (7.4%) exhibited with multiple nodules and 226 (92.6%) presented with single nodules were included in this study. The mean diameter of 289 nodules was  $12.7 \pm 6.4$  cm. If  $SWE\text{-max} \geq 120$  kPa, the nodule was highly suspicious for malignancy. If  $120 > SWE\text{-max} \geq 69$  kPa the nodule was suspicious for malignancy. It indicated that the possibility for malignancy was higher than benignancy. 69 kPa was considered as the expected value for malignant nodules. If  $69 \text{ kPa} > SWE\text{-max} \geq 45$  kPa, the nodule was indeterminate. If  $45 \text{ kPa} > SWE\text{-max}$ , the nodule was suspicious for benignancy.

**Conclusion:** 2D-SWE imaging can provide quantitative information about thyroid nodules' stiffness. And the quantitative parameters are effective in differentiating benign and malignant thyroid nodules.

**Keywords:** Two-dimensional shear wave elastography, Thyroid nodules, Maximum Young's modulus of thyroid nodules.

*Accepted on December 29, 2016*

### **Introduction**

Thyroid nodule is a common clinical disease, about 4%-8% of them can be found by palpation, 68% of which can be detected by high-frequency ultrasound with color Doppler [1]. However, only 5%-15% are malignant. Recently, high-frequency grey-scale ultrasound has played an important role in differentiating malignant from benign nodules. Approved sonographic signs that are suggestive of thyroid malignancy include the following findings: poor margin, irregular shape, taller-than-wide shape, microcalcification, marked hypoechoogenicity, absence of blood flow or peripheral vascularization [2,3]. However, using each single characteristic sign to predict malignancy has relatively low sensitivity (26.5-59.1%) [4,5]. Conventional ultrasonography is very sensitive to thyroid nodules but cannot reliably differentiate the few malignant nodules from the common benign ones [6,7].

By inducing motion in soft tissue, elastography has become a wide medical application field to assess soft tissue mechanical properties. Several techniques appeared according to the type of mechanical properties. Different imaging patterns can be used to estimate the resulting tissue displacements: Ultrasound (US) or Magnetic Resonance (MR). In ultrasound field, US-based elastography, a new technique for soft tissue elasticity mapping, has become a top hot study. It can be widely used in several organs, such as breast, liver, prostate, thyroid, kidney and so on [8-14]. Most malignant thyroid nodules are associated with nodular stiffness, especially for papillary carcinoma which is the most common thyroid cancer type. However, the majority of the benign nodules have a relatively soft texture [15,16]. Therefore, elastography has been considered as a complementary method to help distinguishing malignant from benign thyroid nodules. It has been proved that the quasi-static elastography can help diagnose thyroid nodules

[15,17]. Nevertheless, quasi-static elastography is a qualitative diagnostic tool with many limitations such as relatively low repeatability and high operator dependence. On the other side, as a new quantitative, operator-independent, and reproducible tool, Shear Wave Elastography (SWE) can supplement the conventional ultrasound by quantitative evaluating tissue hardness. The elasticity index delivers quantitative information in terms of shear wave velocity (expressed in m/s) or estimated tissue stiffness (expressed in kilopascals-kPa) [18]. And from the velocity, the Young's modulus is used to impact the tissue stiffness. The harder the tissue is, the higher the Young's modulus [19-21].

Our study was demonstrated to describe the maximum Young's modulus of nodules in discriminating the quality of thyroid nodules.

## Materials and Methods

### *Patients*

This study was approved by the ethics committee of the first affiliated hospital with Nanjing Medical University (2012-SR-058) and opened for enrolment from September 2015 to January 2016. All patients signed a written informed consent. The inclusion criteria included (a) age of 18 years and older; (b) patients who were scheduled to undergo US-guide Fine-Needle Aspiration (FNA) or thyroid surgery; (c) distance from the surface skin to nodule center larger than 2.5 cm; (d) patients had got solid or most solid thyroid nodules by US examination; (e) history of radiotherapy or surgery on head and neck regions and history of previous pharmacotherapy for thyroid nodules were excluded in our study; (f) presence of pure cystic nodules were eliminated [22].

### *US examination*

Thyroid US examinations were performed by a real-time US device (Aixplorer, Supersonic Imagine, Aix en Provence, France) equipped with a linear transducer with 4-15 MHz liner transducer. All the patients accepted grey-scale US and SWE examinations operated by the same operator with more than 3 years' experience in thyroid US and US elastography.

The patients were maintained at a supine position, head backward, fully exposed to the neck. A careful evaluation was performed to get the following grey-scale features for every nodule: echogenicity (remarkable hypoechoic, hypoechoic, isoechoic or hyperechoic in comparison with the adjacent thyroid parenchyma), irregular or regular shape, poor or well margin, absence or presence of halo sign, presence of microcalcifications or mixed calcification (Microcalcifications were defined as calcifications that were 1 mm in diameter, which was visualized as tiny, punctate hyperechoic foci, either with or without acoustic shadows. Macrocalcifications were defined as hyperechoic foci larger than 1 mm, including rim or egg-shell calcifications) [23], aspect ratio and nodular vascularization (absence of blood flow, peripheral vascularisation, increased vascularisation or intranodular blood

flow) [24-28]. Every nodule was classified into different categories according to Kwak [29].

SWE images were obtained for thyroid nodules on longitudinal plane after conventional grey-scale US. The transducer was held without compression or movement when SWE activated. The real-time elastograms were displayed in dual mode alongside grey-scale images to assist in anatomic localization. The region-of-interest (ROI) (Q-box; Supersonic Imagine) was set to cover the nodular lesion and the adjacent normal thyroid parenchyma. On SWE mappings, using a default chromatic scale with succession from blue to red showed soft to hard tissue stiffness. The tissue elastic modulus was showed in kilopascals (kPa) and an upper limit of the display 100 kPa was set. Fixed  $2 \times 2$  mm ROIs were placed over the stiffest part of the nodule, the same level of muscle anterior portion and normal thyroid parenchyma [30]. We acquired at least 3 SWE cine-loops lasting more than 10 s from each lesion for analysis. During SWE examinations, all patients were asked to hold their breath and refrain from other movements at least 3<sup>rd</sup>. The operator froze the image and stored the corresponding image in the machine.

We performed the shear wave elastographic measurement by the Aixplorer, developed by the Supersonic Imagine. We measured the following parameters which were automatically displayed by the machine system: the whole nodule's mean value of EI (SWE-mean), the whole nodule's maximum value of EI (SWE-max), the whole nodule's minimum value of EI (SWE-min), the standard deviation of the EI (SWE-ESD); And all the above indicators were measured when ROIs were covered the nodular lesion and the adjacent normal thyroid parenchyma. Then fixed  $2 \times 2$  mm ROIs to get the following parameters: the normal thyroid's mean value of EI (SWE-mean-thyroid), the normal thyroid's maximum value of EI (SWE-max-thyroid), the muscle anterior portion's mean value of EI (SWE-mean-muscle), the muscle anterior portion's maximum value of EI (SWE-max-muscle). At last, in this study we performed a new index called the E-ratio, which was calculated by the ratio between SWE-max and SWE-max-muscle. On account of the happening of areas lacking SWE signal, the SWE-min was not considered reliable. For each parameter, the measurement was performed at least three times.

All the measurements were performed by at least two operators with more than 3 years' experience in thyroid US and US elastography.

### *Pathologic examination*

All the pathological results, including US-FNA reports and final postoperative diagnosis, were performed by two pathologists with more than 5 years' experience in thyroid according to Bethesda system and WHO guidelines [31]. And all the pathological results were considered as either benignity or malignancy on basis of US-FNA and operative pathological findings.

**Statistical analysis**

We took the average value of three for each parameter's ultimate value. Comparison between the benign and malignant thyroid nodules groups was made by using two independent sample t-test. All the parameters were described as  $\bar{x} \pm S$ , and two-tailed  $p < 0.05$  was considered to be statistically significant. The diagnostic performance for each SWE indices in differentiating benign from malignant thyroid nodules was assessed by Receiver Operating Characteristic (ROC) analyses. Ultimately, the area under the ROC curve (AUC) of SWE-max was the highest one in all the SWE indices. Then we performed analysis of the distribution of the SWE-max by using logarithmic normal distribution. At last we presented a scheme in differentiation the quality of thyroid nodules in accordance with the nodule's SWE-max. We collected all the results in a Microsoft Excel file. The statistical analyses were carried out by using SPSS version 19.0, Medcalc version 10.3.0.0 and Matlab version 7.0.

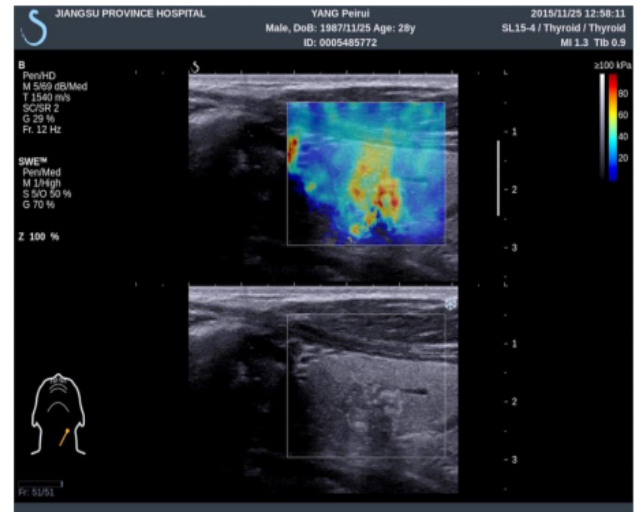


**Figure 2.** SWE image (top) and simultaneous grey-scale image (bottom) in a 28-year-old male. The 2D-SWE mapping showed a yellow even red area representing high Young's modulus, and the nodule was diagnosed as a malignant papillary carcinoma at surgical pathologic investigation.

**Results**

At last, 24 patients with 29 nodules were yielded because of non-diagnostic results after US-FNA (Bethesda category I). Overall, 244 patients (197 female and 47 male) with 289 nodules acquiring specific pathological results were recruited in our study. The mean age was  $45.58 \pm 12.15$  years old (range from 21 to 76 years). Of all these 244 patients, 18 (7.4%) exhibited with multiple nodules and 226 (92.6%) presented with single nodules were included in this study. The mean diameter of 289 nodules was  $12.7 \pm 6.4$  cm, range from 0.3 to 3.9 cm. The final pathological results were obtained from US-FNA and surgical specimens. For most thyroid nodules, the 2D-SWE mapping showed a homogeneous blue pattern representing low Young's modulus in benign ones and an in homogeneous pattern with yellow even red area for malignant ones (Figure 1). And all the pathological results were summarized in Table 1.

**Grey-scale US examinations**

We performed the main signs' statistical analyses of conventional ultrasound in diagnosing thyroid nodules. Comparison between the benign and malignant thyroid nodules groups was made by using two independent sample t-test. Then we drew ROC curve of each criteria, got the AUC value, sensitivity and specificity. And all the results were collected in Table 2.

Among all the grey-scale features, irregular shape was the best characteristic to predict malignant thyroid nodule (75.3% sensitivity and 74.8% specificity,  $p=0.04$ ). Hypoechogenicity was the highest sensitivity (98.2%) to diagnose malignancy, but the specificity was extremely low (only about 19.3%),  $p=0.000$ . Taller-than-wide shape was considered to be the highest

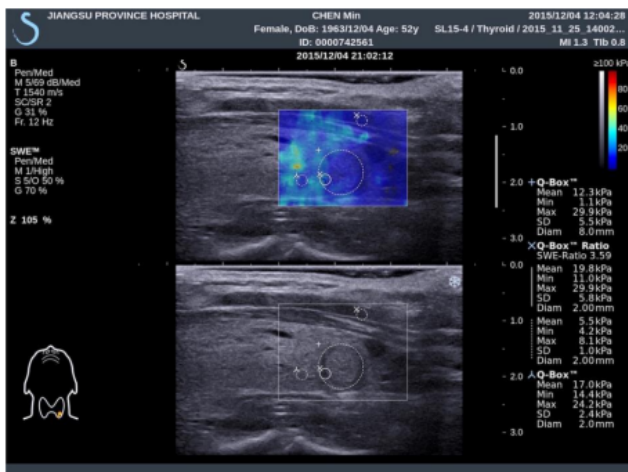


**Figure 1.** SWE image (top) and simultaneous grey-scale image (bottom) in a 52-year-old female. The 2D-SWE mapping showed a homogeneous blue pattern representing low Young's modulus, and the nodule was diagnosed as a benign follicular adenoma at surgical pathologic investigation.

**Table 1.** Distribution of 289 thyroid nodules according to pathology.

Pathological results	n	
Malignant	Papillary carcinoma	168
	Medullary carcinoma	2
	Total	170
Benign	Nodular goitre	43
	Adenoma	68
	Hashimoto's thyroiditis	5
	Focal thyroiditis	3
	Total	119
	Total	289

specificity (94.1%) feature in differentiating thyroid nodules, but the sensitivity was also very low (about 22.9%),  $p=0.000$ .

**Table 2.** Diagnostic performance of grey-scale US signs in differentiating thyroid nodules.

		Pathology		p	AUC	Sensitivity (%)	Specificity (%)
		Benign	Malignant				
Shape	Oval	89	42	0.004	0.758	75.3	74.8
	Roundness	9	28				
	Irregular	21	100				
Aspect ratio	>1	7	39	0	0.585	22.9	94.1
	<1	112	131				
Margin	Well	98	58	0	0.74	65.5	82.4
	Poor	21	112				
Boundary	Closely linked	95	158	0.001	0.562	92.9	20.2
	Halo sign	24	12				
Echogenicity	Mixed-echogenicity	18	12	0	0.527	98.2	19.3
	Hypoechoicity	74	152				
	Isoechoicity	23	3				
	Hyperechoicity	4	3				
Calcification	Absence	97	63	0	0.741	59.9	89
	Microcalcification	14	103				
	Large calcification	8	4				
Vascularisation	Absence of blood flow	27	54	0.117	0.565	31.8	77.3
	Peripheral vascularisation	18	2				
	Increased vascularisation	74	114				

**SWE examinations**

**Quantitative measurement:** The main signs’ statistical analyses were performed with SWE elasticity indices between benign and malignant thyroid nodules. And the comparison was made by using two independent sample t-test. We mapped all the SWE quantitative parameters’ ROC curve, got their AUC value, sensitivity and specificity. All the results were collected in Table 3.

Among all the parameters, SWE-max was considered to be the most effective one to differentiating benign and malignant thyroid nodules ( $p=0.000$ ). And 52.7 kPa was considered to be a cut-off value in diagnosing thyroid nodules. But this cut-off

value was based on a normally distributed data. In previous articles, a normally distributed data was rarely mentioned. So we drew a statistical distribution histogram about SWE-max. The column diagram showed in Figure 2. The SWE-max’s distribution range was showed in Table 4.

From Figure 2, we could see clearly that the SWE-max was abnormally distributed. Using statistics of normal distribution assumption of statistical procedure, the result of the test was not in conformity with the real data distribution. So the result was unreasonable. And this might be the reason for bad result statistics of thyroid nodules.

**Table 3.** Diagnostic performance of SWE elasticity indices between benign and malignant thyroid nodules.

	Benign	Malignant	P value	AUC	Sensitivity (%)	Specificity (%)
SWE-mean	23.2 ± 9.6	30.4 ± 10.5	0	0.741	72.9	70
SWE-max	50.9 ± 26.0	75.9 ± 38.8	0	0.764	75.3	73.1

*Investigation of the maximum Young's modulus of thyroid nodules using two-dimensional shear wave elastography in thyroid nodules*

SWE-mean-muscle	16.0 ± 3.9	16.6 ± 4.4	0.179	---	---	---
SWE-mean-thyroid	14.0 ± 4.3	14.3 ± 4.5	0.581	---	---	---
E-ratio	2.73 ± 3.33	3.37 ± 2.17	0.048	0.585	22.9	94.1

**Table 4.** Distribution range of SWE-max between benign and malignant thyroid nodules.

E <sub>max</sub>	Maximum (kPa)	Minimum (kPa)
Malignant nodules	271.5	22.7
Benign nodules	186.5	18.1

**The probability analysis of SWE-max**

It was considered to be a peak near 40 kPa in Figure 2. The SWE-max was in small range below 40 kPa, and there would be a threshold value near 18 kPa. This threshold value was considered to be the Young's modulus of normal thyroid parenchyma. It was slowly declined when the SWE-max was above 40 kPa. And this distribution of thyroid nodules' SWE-max was in accordance with the previous studies. So we used a logarithmic normal distribution of SWE-max according to the frequency distribution. We drew a probability density function curve and got expected value of two-kinds of thyroid nodules (Figure 3). All the statistical results were collected in Table 5.

**Table 5.** SWE-max's statistical result of benign and malignant thyroid nodules.

Statistical parameter	Number of data points	Expected values E		Variance yields σ
		Lg (x)	X (kPa)	
Malignant nodules	170	4.235	69.1	0.4465
Benign nodules	119	3.812	45.2	0.4297

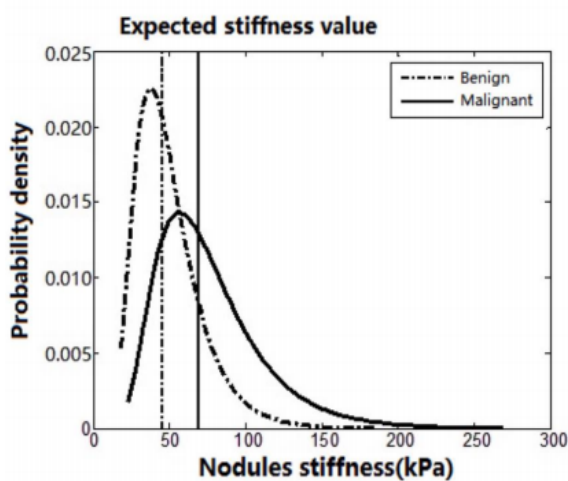


**Figure 3.** Probability density function curve and expected value of two-kinds of thyroid nodules.

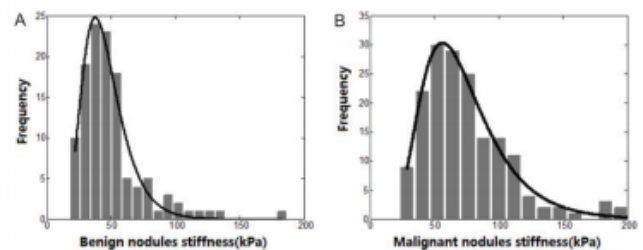


**Figure 4.** Logarithmic normal distribution of thyroid nodules (A): Stiffness of benign nodules; (B): Stiffness of malignant nodules.

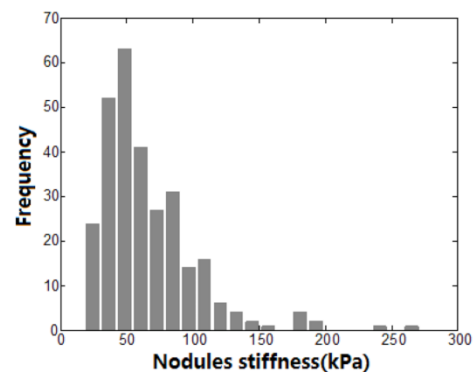


**Figure 5.** SWE-max's statistical distribution histogram.

**Discussion**

Thyroid malignant nodules, as a majority of them are papillary thyroid carcinomas, most of them are hard. The stiffness evaluation has become part of nodules characterization. US elastography, a recent and sophisticated imaging technique, has been considered to evaluate tissue stiffness [28]. Real-time shear wave elastography (Supersonic Elastography, SSE) is a new elastic technical developed in recent years. It is an operator-independent, reproducible and quantitative elastography method [29,30]. The elastography imaging is overlaid on the grey-scale image. Its inter- and intra-operator reproducibility in quasi-static elastography is acceptable, with a correlation coefficient ranging from 0.73 to 0.79 for inter-observer variability and between 0.73 and 0.84 for intra-observer variability [31]. Up to now, some studies using SSE to assess thyroid nodules, trying to differentiating benign vs. malignant by define a cut-off value of the Elasticity Index (EI). A closest study, made by Park et al. [32], reported that a mean value for EI ≥ 85 kPa or a maximum value ≥ 94 kPa are independent predictors of thyroid malignancy [33]. All the reported cut-off value was different from each other. And Bathia et al. [34] calculated different cut-off values for EI, with the ROI kept at 2 mm, found that increasing the cut-off value

(>10.3 kPa, >132 kPa) is associated with increasing specificity (8.9-100%), and decreasing sensibility (100-7.7%). And all the studies used normal distribution model. In our study, we could see clearly from Figure 3 that the SWE-max was abnormally distributed. Using statistics of normal distribution assumption of statistical procedure, the result of the test was not in conformity with the real data distribution. So, it is obviously inaccurate to differentiating benign vs. malignant by define a cut-off value of the Elasticity Index (EI).

Therefore, we used a logarithmic normal distribution model in our study. And this kind of model could best reflex thyroid nodules' maximum Young's modulus, being characteristic of asymmetric distribution and bad concentration. In logarithmic normal distribution models, the expected value was different from peak value. So, the SWE-max's distribution character could be better reflected by the logarithmic normal distribution model. Taking malignant thyroid nodules for instance (Figures 4 and 5), the centrostigma point of the SWE-max's distribution or the peak value of the probability density function was around 57 kPa. But the mean value of SWE-max or the expected value of the logarithmic normal distribution was around 69 kPa.

A total of 289 thyroid nodules were enrolled in our study, and 119 nodules were benign (41.2%), 170 nodules were malignant (58.8%). And this kind of statistical distribution was reliable

**Table 6.** Distribution range of SWE-max for differentiating thyroid nodules.

$E_{max}$ (kPa)	$E_{max} \geq 120$	$120 > E_{max} \geq 69$	$69 > E_{max} \geq 45$	$E_{max} < 45$
Thyroid nodules	Highly suspicious for malignancy	Suspicious for malignancy	Indeterminate	Suspicious for benignancy

**Table 7.** Distribution of 289 thyroid nodules according to pathological results and distribution range.

$E_{max}$ (kPa)	Total	Number	
$E_{max} \geq 120$	19	Benign	1
		Malignant	18
$120 > E_{max} \geq 69$	84	Benign	14
		Malignant	70
$69 > E_{max} \geq 45$	95	Benign	34
		Malignant	61
$E_{max} < 45$	90	Benign	76
		Malignant	14

We collected our data in Table 7 according to the  $E_{max}$  distribution range. From Table 7 we could see only one benign thyroid nodule's  $E_{max}$  value was higher than 120 kPa. After we reviewed this image data, this nodule was larger than two centimetres with no calcification. And the distance from nodule to the body surface was only 5 mm. So the pressure applied on the neck from the nodule might alter the values of EI [35]. In other words, the closer distance to the body surface of nodules and the bigger nodules got higher EI values. In our

for statistical result. It was obviously that the SWE-max of malignancy was higher than benignancy. So the SWE-max could be as an auxiliary pointer in diagnosing thyroid nodules. Totally speaking, we presented a distribution range of SWE-max for differentiating thyroid nodules. The results were collected in Table 6. And the distribution range was as follows:

If  $SWE-max \geq 120$  kPa, the nodule was highly suspicious for malignancy. And the possibility of SWE-max was less than 2% in benign nodules.

If  $120 > SWE-max \geq 69$  kPa the nodule was suspicious for malignancy. It was mean that the possibility for malignancy was higher than benignancy. 69 kPa was considered as the expected value for malignant nodules. Among this range, the possibility of SWE-max in malignant nodules was higher than 50%, but slim chance appeared in benign nodules.

If  $69 > SWE-max \geq 45$  kPa, the nodule was indeterminate. In other words, when the SWE-max was in this range, the nodules were considered to both in possible.

If  $45 > SWE-max$ , the nodule was suspicious for benignancy. It was mean that the possibility for benignancy was higher than malignancy. There was less chance for malignant nodules for reaching such a low SWE-max value, but the possibility of benign nodules was around 50%.

study, 90 nodules'  $E_{max}$  value was under 45 kPa including 14 malignant nodules. After we had a retrospective analysis of these nodules, all the 14 malignant nodules' size was less than or equal to 1 cm. Two nodules contained microcalcifications among the 14 nodules had bigger EI values than the rest ones. So, a malignant nodule equal or less than 1 cm in maximum diameter got lower EI values than the bigger nodules. And this result was similar to Liu et al. [36]. In a word, nodule size, presence of calcification and distance between body surface to the nodule were limitations of performing SSE in thyroid nodules [37,38].

At last, we could see from Table 6 that our results were similar to the thyroid imaging reporting and data system proposed by Kwak [19]. So we could combine our results with the thyroid imaging reporting and data system for US features of nodules.

The shear wave elastography imaging can provide quantitative information about thyroid nodules' stiffness. And the quantitative parameters are effective in differentiating benign and malignant thyroid nodules. Our results are similar to the thyroid imaging reporting and data system. We could combine our results with the thyroid imaging reporting and data system for US features of nodules. Finally, we enrolled SWE-max as a single index for differentiating benign and malignant thyroid

## *Investigation of the maximum Young's modulus of thyroid nodules using two-dimensional shear wave elastography in thyroid nodules*

nodules in this study. The analysis of other parameters and combined application of them were not evaluated in our study.

### **Acknowledgements**

We thank the financial support from Shanghai General Hospital of Nanjing Medical University.

### **Conflict of Interest**

None

### **References**

1. Tunbridge WM, Evered DC, Hall R, Appleton D, Brewis M, Clark F, Evans JG, Young E, Bird T, Smith PA. The spectrum of thyroid disease in a community: the Wickham survey. *Clin Endocrinol* 1997; 7: 481-493.
2. Lagalla R, Caruso G, Romano M, Midiri M, Novara V. Echo-color Doppler in thyroid disease. *Radiol Med* 1993; 85: 109-113.
3. Messina G, Viceconti N, Trinti B. Echotomography and color-Doppler in the diagnosis of thyroid carcinoma. *Ann Ital Med Int* 1996; 11: 263-267.
4. Katz JF, Kane RA, Reyes J, Clarke MP, Hill TC. Thyroid nodules: sonographic-pathologic correlation. *Radiology* 1984; 151: 741-745.
5. Solbiati I. Thyroid gland. *Diagnostic Ultrasound*. St.Louis: Mosby (2nd edn.) 1998; 703-729.
6. Gharib H, Papini E, Paschke R, Duick DS, Valcavi R, Hegedus L, Vitti P. American Association of Clinical Endocrinologists, Associazione Medici Endocrinologi and European Thyroid Association medical guidelines for clinical practice for the diagnosis and management of thyroid nodules: executive summary of recommendations. *J Endocrinol Invest* 2010; 33: 51-56.
7. Gharib H, Papini E, Paschke R. American Association of Clinical Endocrinologists, Associazione Medici Endocrinologi and European Thyroid Association Medical Guidelines for Clinical Practice for the Diagnosis and Management of Thyroid Nodules. *Endocr Pract* 2010; 16: 1-43.
8. Liu BX, Xie XY, Liang JY, Zheng YL, Huang GL. Shear wave elastography versus real-time elastography on evaluation thyroid nodules: a preliminary study. *Eur J Radiol* 2014; 83: 1135-1143.
9. Evans A, Whelehan P, Thomson K, McLean D, Brauer K, Purdie C, Baker L, Jordan L, Rauchhaus P, Thompson A. Invasive breast cancer: relationship between shear-wave elastographic findings and histologic prognostic factors. *Radiology* 2012; 263: 673-677.
10. Ferraioli G, Tinelli C, Dal Bello B, Zicchetti M, Filice G, Filice C. Accuracy of real-time shear wave elastography for assessing liver fibrosis in chronic hepatitis C: a pilot study. *Hepatology* 2012; 56: 2125-2133.
11. Foucher J, Chanteloup E, Vergniol J, Castéra L, Le Bail B. Diagnosis of cirrhosis by transient elastography (FibroScan): a prospective study. *Gut* 2006; 55: 403-408.
12. Kwon HJ, Kang MJ, Cho JH, Oh JY, Nam KJ, Han SY, Lee SW. Acoustic radiation force impulse elastography for hepatocellular carcinoma-associated radiofrequency ablation. *World J Gastroenterol* 2011; 17: 1874-1878.
13. Garra BS. Elastography: current status, future prospects, and making it work for you. *Ultrasound Q* 2011; 27: 177-186.
14. Lee SH, Chang JM, Kim WH, Bae MS, Cho N, Yi A, Koo HR, Kim SJ, Kim JY, Moon WK. Differentiation of benign from malignant solid breast masses: comparison of two-dimensional and three-dimensional shear-wave elastography. *Eur Radiol* 2013; 23: 1015-1026.
15. Shuzhen C. Comparison analysis between conventional ultrasonography and ultrasound elastography of thyroid nodules. *Eur J Radiol* 2012; 81: 1806-1811.
16. Tae HJ, Lim DJ, Baek KH, Park WC, Lee YS, Choi JE, Lee JM, Kang MI, Cha BY, Son HY, Lee KW, Kang SK. Diagnostic value of ultrasonography to distinguish between benign and malignant lesions in the management of thyroid nodules. *Thyroid* 2007; 17: 461-466.
17. Wang Y, Dan HJ, Dan HY, Li T, Hu B. Differential diagnosis of small single solid thyroid nodules using real-time ultrasound elastography. *J Int Med Res* 2010; 38: 466-472.
18. Sebag F, Vaillant-Lombard J, Berbis J, Griset V, Henry JF, Petit P, Oliver C. Shear wave elastography: a new ultrasound imaging mode for the differential diagnosis of benign and malignant thyroid nodules. *J Clin Endocrinol Metab* 2010; 95: 5281-5288.
19. Kwak JY, Han KH, Yoon JH, Moon HJ, Son EJ, Park SH, Jung HK, Choi JS, Kim BM, Kim EK. Thyroid imaging reporting and data system for US features of nodules: a step in establishing better stratification of cancer risk. *Radiology* 2011; 260: 892-899.
20. Tanter M, Bercoff J, Athanasiou A. Quantitative assessment of breast lesion viscoelasticity: initial clinical results using supersonic shear imaging. *Ultrasound Med Biol* 2008; 34: 1373-1386.
21. Bercoff J, Tanter M, Fink M. Supersonic shear imaging: a new technique for soft tissue elasticity mapping. *IEEE Trans Ultrason Ferroelectr Freq Control* 2004; 51: 396-409.
22. Seriei S, Orell F. The rational mechanics of flexible or elastic bodies 1638-1788. *Opera mechanica et astronomica* 1960: 10.
23. Liu B, Liang J, Zheng Y, Xie X, Huang G, Zhou L, Wang W, Lu M. Two-dimensional shear wave elastography as promising diagnostic tool for predicting malignant thyroid nodules: a prospective single-centre experience. *Eur Radiol* 2015; 25: 624-634.
24. Appetecchia M, Solivetti FM. The association of colour flow Doppler sonography and conventional ultrasonography improves the diagnosis of thyroid carcinoma. *Horm Res* 2006; 66: 249-256.

25. Ozel A, Erturk SM, Ercan A, Yalmaz B, Basak T. The diagnostic efficiency of ultrasound in characterization for thyroid nodules: how many criteria are required to predict malignancy? *Med Ultrason* 2012; 14: 24-28.
26. Horvath E, Majlis S, Rossi R. An ultrasonogram reporting system for thyroid nodules stratifying cancer risk for clinical management. *J Clin Endocrinol Metab* 2009; 94: 1748-1751.
27. Liang XN, Guo RJ, Li S. Binary logistic regression analysis of solid thyroid nodules imaged by high-frequency ultrasonography, acoustic radiation force impulse, and contrast-enhanced ultrasonography. *Eur Rev Med Pharmacol Sci* 2014; 18: 3601-3610.
28. Shao J, Shen Y, Lu J, Wang J. Ultrasound scoring in combination with ultrasound elastography for differentiating benign and malignant thyroid nodules. *Clin Endocrinol (Oxf)* 2015; 83: 254-260.
29. Kwak JY, Jung I, Baek JH. Image reporting and characterization system for ultrasound features of thyroid nodules: multicentric Korean retrospective study. *Korean J Radiol* 2013; 14: 110-117.
30. Heidinger CHR, Sobin LH. Histological typing of thyroid tumors. In: World health Organization, editor. *International histological classification of tumors*. Geneva: Roto Satag AS 1974; 17-27.
31. Slapa RZ, Piwowonski A, Jakubowski WS, Bierca J, Szopinski KT, Slowinska-Srzednicka J, Migda B, Mlosek RK. Shear wave elastography may add a new dimension to ultrasound evaluation of thyroid nodules: case series with comparative evaluation. *J Thyroid Res* 2012; 2012: 657147.
32. Hegedus L. Can elastography stretch our understanding of thyroid histomorphology? *J Clin Endocrinol Metab* 2010; 95: 5213-5215.
33. Sebag F, Vaillant-Lombard J, Berbis J, Griset V, Henry JF. Shear wave elastography: a new ultrasound imaging mode for the differential diagnosis of benign and malignant thyroid nodules. *J Clin Endocrinol Metab* 2010; 95: 5281-5288.
34. Lim DJ, Luo S, Kim MH, Ko SH, Kim Y. Interobserver agreement and intraobserver reproducibility in thyroid ultrasound elastography. *AJR Am J Roentgenol* 2012; 198: 896-901.
35. Park AY, Son EJ, Han K, Youk JH, Kim JA. Shear wave elastography of thyroid nodules for the prediction of malignancy in a large scale study. *Eur J Radiol* 2015; 84: 407-412.
36. Bhatia KS, Tong CS, Cho CC, Yuen EH, Lee YY, Ahuja AT. Shear wave elastography of thyroid nodules in routine clinical practice: preliminary observations and utility for detecting malignancy. *Eur Radiol* 2012; 22: 2397-2406.
37. Ying L, Panghan C, Xiukun W. Health-related quality of life of Chinese earthquake survivors: a case study of five hard-hit disaster counties in Sichuan. *Soc Ind Res* 2014; 119: 943-966.
38. Ying L, Runxia C. Employment assistance policies of Chinese government play positive roles. The impact of post-earthquake employment assistance policies on the health-related quality of life of Chinese earthquake populations. *Soc Ind Res* 2015; 120: 835-857.

#### \*Correspondence to

Lian-fang Du

Department of Ultrasound

Shanghai General Hospital of Nanjing Medical University

PR China